Referee Comment #2

We would like to thank the anonymous referee for taking the time to carefully read the submitted paper and for commenting it. The comments were very useful for improving the readability and effectiveness of our paper. In the following, answers to comments are reported in italics, just below each related comment. The comments are underlined and numbered to ease the process. When needed, the part of the manuscript we modified or added to the old version is reported in bold. Moreover, the references are given in the end of the document.

1. Section 2.2.1 to 2.2.5: You show an extensive overview of the intensive optical properties for the different aerosol types. However, it would be valuable if you could provide further information if the different intensive properties have been derived from the same studies. For using those in the classification the influence of miss-classifications and mixtures should be minimized and the measurements providing a multitude of intensive optical properties should have a larger weight. Additionally you overview mainly focuses on the information presented by Burton et al. or from EARLINET measurements. It would be also valuable to include further measurements (e.g. closer to source regions or after long-range transport) to better differentiate between possible influences of transport or mixture.

The proposed methodology aims to be an EARLINET stand-alone typing methodology. EARLINET collected observations, since 2000, provide an insight of the aerosol types occurring over Europe. Therefore, the methodology is set up and the aerosol classes defined. The aerosol properties are shown to vary with location and aerosol type. For example, as reported also in the paper, desert dust can have different properties depending on the source region (Arabian versus Saharan dust particles). This means that the automatic typing can be more efficient if set up at regional/continental level.

On this basis, Section 2.2 gives an overview of the characteristics of each aerosol type along with intensive optical properties from various literature references. The goal of this section is to introduce the aerosol classes that the automatic typing is based upon and to provide typical values of the intensive parameters. These intensive parameters correspond to the selected classifying parameters and act as a reference to our training dataset. Besides, the majority of the literature references come from EARLINET observations and reflect the variability of the aerosol properties over Europe. The overall performance of the automatic typing is based on the quality of the reference dataset and the definition of coherent aerosol classes. For the reference dataset, well-characterized EARLINET data from Pappalardo et al. (2013), Papagiannopoulos et al. (2016), and Schwarz (2016) were used. The aerosol classification follows the procedure described in Section 2.1. The aerosol classes coincide with the typical values of the Section 2.2 (see Page 27 – Table 2).

The algorithm has been shown to be versatile and can be adjusted to the needs of each study. The reference dataset can be enlarged with well-characterized observations and increase the number of instances of under-represented aerosol classes. In addition, new aerosol classes can be added to describe other aerosol mixtures or the aerosol classes can be redefined. For example, an aerosol class Arabian dust can be inserted in the reference dataset in order to take into account of the different characteristics of the generating desert source.

The next paragraph is inserted in Section 2.2:

As an additional consideration, the defined aerosol types presented in Sect. 2.2 may not be representative of the entire aerosol load and, furthermore, apart from the dust mixtures they do not consider other aerosol mixtures. For example, this aspect can be observed in the definition of the volcanic category where the particles have different characteristics depending the transport pattern. The particles near the source have

optical properties similar to desert dust whereas long-range transported volcanic plumes have the altered properties due to the sedimentation of the coarser particles. Therefore, it is important to further include a more exhaustive aerosol class analysis.

2. Figure 2: Why do you show profiles below the full overlap of the lidar when you do not use them for your analysis? How trustworthy are the values in these height levels? What is meant by the statement 'the layers present the same behavior'? Looking at the profiles at different wavelengths I would suggest having different behaviors at different height levels, e.g. the wavelength dependence of the backscatter coefficient, the lidar ratio and the shape of the lidar ratio between 1.8 and 2 km is different to the height range between 2 and 3.6 km, above 3.6 km the Angstroem exponent of the extinction coefficient shows a different values than below.

The overlap height is at around 1,15 km a.s.l. for 1064 nm (Madonna et al., 2015). Values below the overlap region are not shown. We do not take into account values below the full overlap and the constructed database does not suffer from overlap issues whatsoever.

In the revised version of the paper we rephrased the sentence because it is actually misleading. The referee is right that three different layers are observed as reported in P5L19-20. The layer mean intensive parameters are given in Table A. The Ångström exponent for the 3 layers maintains a rather stable character with values around 0 suggesting large particles over Potenza. Regarding the lidar ratio, the values decrease with height and confirm the comment that we should not consider a single aerosol type throughout the range.

Table A: *the mean intensive parameters for the 3 layers observed.*

Layer[km]	$\kappa_\beta(355,532)$	$\kappa_\beta(532,1064)$	$\kappa_\beta(355,1064)$	$\kappa_\alpha(355,532)$	S_{355} [sr]	S_{532} [sr]
1.6-2.0	*0.45±0.03*	*0.32±0.03*	*0.37±0.02*	*-0.2±0.2*	*53±8*	*57±8*
2.0-3.5	*-0.02±0.12*	*0.42±0.06*	*0.26±0.04*	*-0.3±0.2*	*48±4*	*53±4*
3.5-5.0	*0.12±0.26*	*0.42±0.18*	*0.31±0.13*	*0.4±0.2*	*46±8*	*41±5*

Besides, we investigated the backward trajectories for the layers of Table A using the HYSPLIT model (Stein et al., 2015). We initiated the model for a 7-day backward analysis and starting height levels the midpoints of the layers and the results are shown in Figure A. The layers 2.0-3.5 km and 3.5-5 km show a similar pattern with the air-masses flying over 2 km and originate from the Saharan desert. The layer 1.6-2.0 km follows a different pathway, the air-masses circulate over the Mediterranean Sea and Algeria and the uptake of marine particles is very likely. This information combined with the information of Table A suggests dust particles for the 2 elevated layers.

However, it is right to mention here that this case is reported for showing how the identification is done using intensive properties and backward trajectory analysis. All the intensive properties used for setting up the training and testing datasets are related to elevated layers separated from the planetary boundary layer and the local influence.

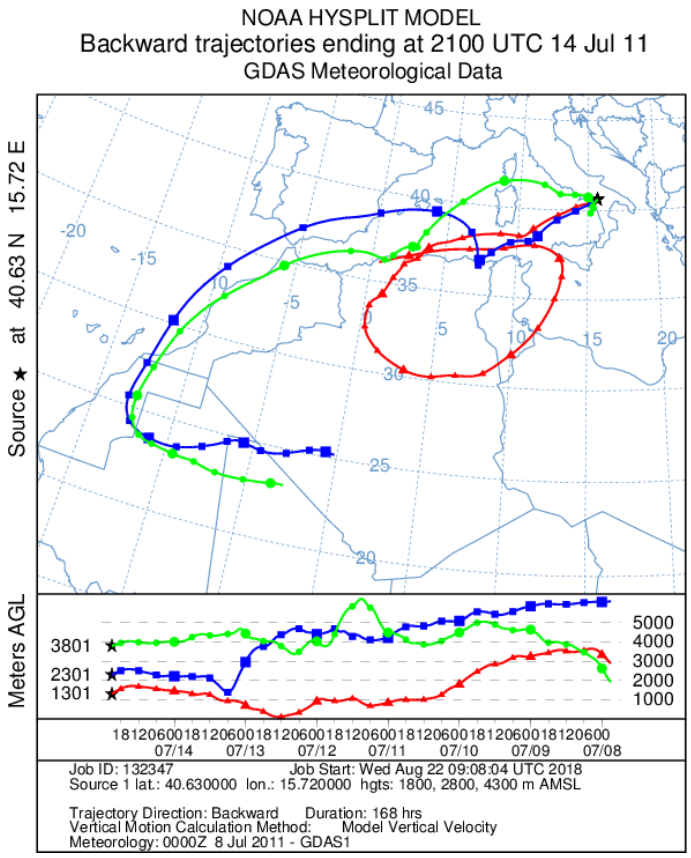

Figure A: *HYSPLIT backward trajectories for the aerosol layers observed over Potenza, on 14 July 2011, 19:20–22:10 UTC.*

In synthesis, the 3 layers with the synergistic use of intensive properties and backward trajectory analysis allows us to distinguish the different characteristics of the mixed dust layer in the range 1.6-2.0 km and the desert dust higher in the atmosphere (2.0-5.0 km). The intensive properties are measured with good level of uncertainty only in the layer 2.0-3.5 km. In order to avoid confusion, we will focus our comments in the range 2.0-3.5 km where the intensive property analysis is coherent and confirms the existence of a dust layer. The text implemented in P5L22-24 is given below:

The layer 2.0-3.5 km has a constant behavior with the range for the intensive optical profiles indicating the presence of the same type of particles. The mean values of all optical parameters in the range are calculated: lidar ratios of 48±4 sr at 355 nm and 53±4 sr at 532 nm and Ångström exponents of -0.3–0.4 were found.

3. Figure 3: Looking at the FLEXPART footprint, can you exclude a contribution from marine aerosols?

The manual typing as described in Section 2.1 is not a simple issue and, of course, leaves room to questionable type assignment. The backward trajectory analysis is used synergistically with the lidar optical properties and the model outputs suffer from the high error on the path (increasing with the path itself) and the source term assignment. Therefore, the model simulations have to be used together with the observed lidar optical properties for providing a reasonable aerosol typing.

The FLEXPART seems to indicate the possibility of marine influence in the identified layer, however the lidar ratio values being over 50 sr indicates low or no presence of maritime aerosol particles. Furthermore, for this specific case, particle linear depolarization ratio measurements are available, however these measurements are not included in the database and therefore not reported in the submitted manuscript. Figure B shows the particle

linear depolarization ratio where the values are over 0.2 and, thus, confirming our hypothesis of aspherical particles.

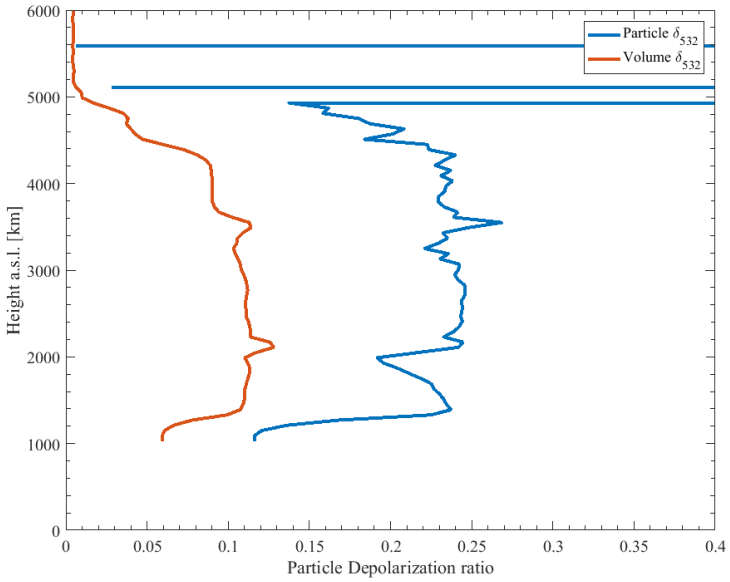

Figure B: *Particle (blue line) and Volume (red line) linear depolarization ratio at 532 nm for the MUSA system in Potenza on 14/07/2011, 19:20–22:10 UTC.*

In order to avoid confusion, we rephrased the sentence following the referee's comment in P5L30-31 and moved P5L24-25 to the end of it:

The dust-prone area of northern Africa (Morocco and northern Algeria) along with the Mediterranean Sea are most likely the sources of the observed layer and suggest a mixture of dust and marine particles. The combined information of the backward trajectory analysis and the intensive properties values indicate the presence of dust particles and they are in accordance with the typical dust values observed over Potenza (Mona et al., 2014).

4. Figure 5: An additional Figure also including the information of the depolarization ratio for the different classes would be valuable.

Figure C shows the characteristics of the reference dataset in terms of the depolarization ratio when plotted against the lidar ratio at 532 nm and the backscatter related Ångström exponent (355,1064) for 8 aerosol classes. The particle depolarization ratio values were assigned to the aerosol classes assuming that the intensive properties are normally distributed and using literature values as reported in P29-Table 4. Therefore, the values have no standard deviation. The figures highlight the discriminatory power of the classifying parameter among the dust-like aerosol classes, however, the particle depolarization ratio seems to have no power to separate the non-dust classes.

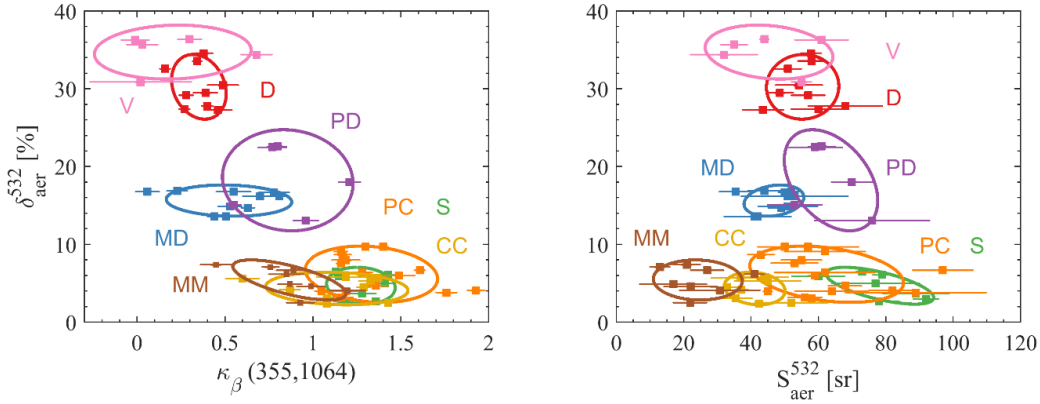

***Figure C**: Colored pre-specified classes and 90 % confidence ellipses for 8 aerosol classes using the classifying parameters: δ_{532}, S_{532}, $\kappa_\beta(355,1064)$. The error bars correspond to the standard deviation of the selected mean intensive properties. CC stands for Clean Continental, D stands for dust, MD stands for mixed dust, MM stands for mixed marine, PD stands for polluted dust, PC stands for polluted continental, S stands for smoke, and V stands for volcanic particles.*

In conjunction with the specific comment #9 of RC1, we inserted in the revised manuscript Figure D and the text below in Section 3.2.4:

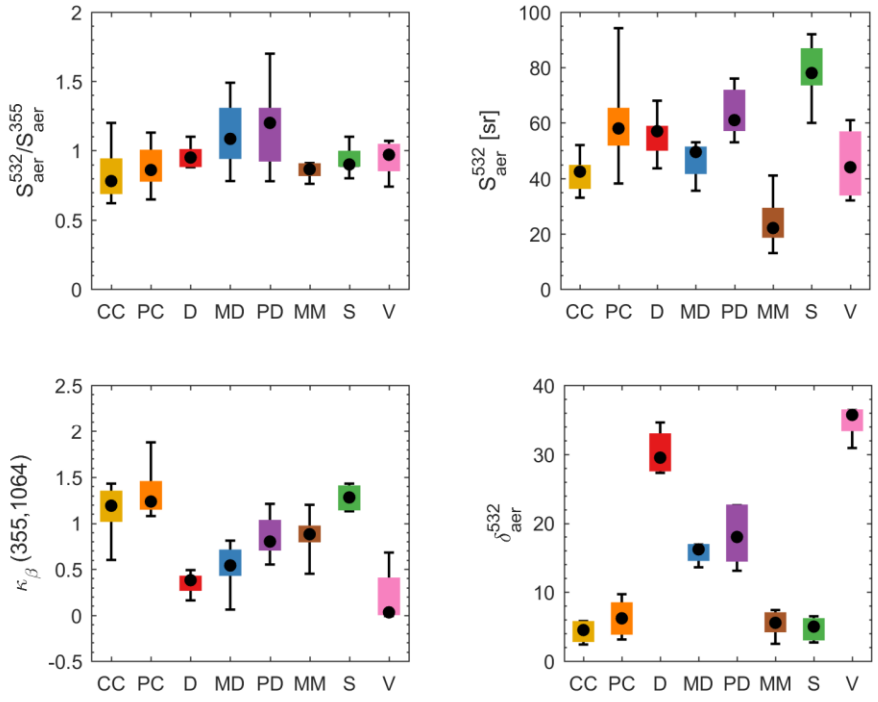

***Figure D:** Bar plots show the median (horizontal line), 25-75 percentile (box) and 5-95 percentile (whisker) of the four classifying parameters: δ_{532}, $\kappa_\beta(355;1064)$, S532, and S_{532}/S_{355}. CC stands for Clean Continental, D stands for dust, MD stands for mixed dust, MM stands for mixed marine, PD stands for polluted dust, PC stands for polluted continental, S stands for smoke, and V stands for volcanic particles.*

Figure 7 presents cumulative barplots with the median (black dots), the 25-75 percentile (box), the 5-95 percentile (whiskers) for all 4 classifying parameters. The figure highlights the discriminatory power of δ_{532}, $\kappa_{\beta}(355,1064)$, and S_{532}, whereas the S_{532}/S_{355} performs the worst. Furthermore, the figure depicts the discriminatory power of the classifying parameter among the dust-like aerosol classes, however, the particle depolarization ratio seems to have no power to separate the non-dust classes, as discussed above.

5. Figure 7: The shape of the backscatter coefficient and the extinction coefficient at 355 and at 532 nm show different shapes, but the derived profile of the lidar ratio for both wavelengths shows the same shape. What is the vertical resolution of the different profiles? Did the extinction and backscatter coefficient have the same resolution for deriving the lidar ratio?

P34-Figure 2 and P39-Figure 7 in the submitted paper are reporting the profiles at their highest resolutions, i.e. the particle backscatter coefficient profiles have a higher resolution when compared to the particle extinction coefficient ones and typically ultraviolet profiles have a better resolution than visible profiles. The lidar ratio profiles have the same resolution of the particle extinction coefficient profiles. Prior to the calculation of the lidar ratio, the particle backscatter coefficient profiles are smoothed using a 2nd order Savitzky-Golay filter at an effective vertical resolution that varies with height, for more details see Iarlori et al. (2015).

In particular, for P34-Figure 7, the vertical raw resolution of the particle backscatter coefficient profiles is 7.5 m while for the extinction coefficient the resolution varies with height. The effective resolution for 355 nm (blue line) and 532 nm (red line) is given in Figure E and follows the procedure described in Pappalardo et al. (2004). For the height range 1.2-1.9 km, the highest resolution is 240 m for 355 nm while for 532 nm varies from 240 m to 480 m. Higher in the atmosphere, the resolution degrades with height (faster for 532 nm) and becomes constant at 4.7 km for 355 nm (3.8 km for 532 nm).

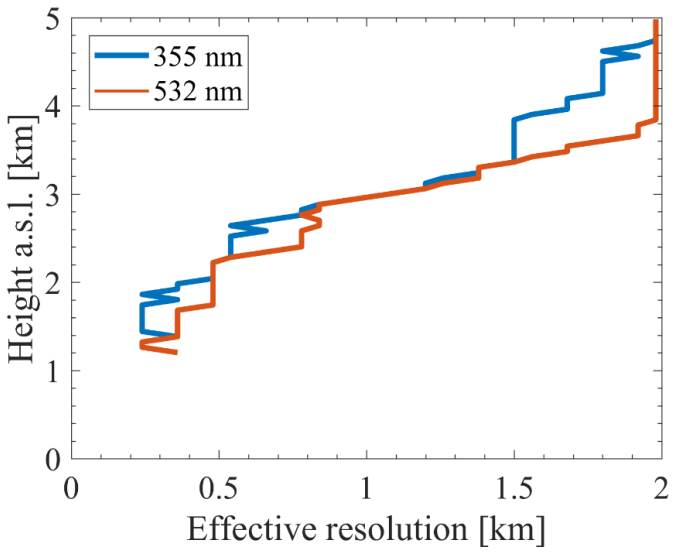

Figure E: *The effective resolution of the extinction coefficient at 355 nm (blue line) and 532 nm (red line) for the Athens lidar on 22/05/2014, 20:28–21:28 UTC.*

Figure F shows the same panels as for P34-Figure 7 along with the smoothed backscatter profiles (panel b) that were used for the calculation of the lidar ratio. The next sentence is implemented in the revised manuscript:

The particle extinction and backscatter coefficient are given with their full resolution. To calculate the lidar ratio, the backscatter coefficient was smoothed in the same effective vertical resolution using a Savitzky-Golay

second order filter (Iarlori et al., 2015) and only the useful range of signals was kept; the effective resolution of the resulting profiles varied from 240 m to 780 m using the method described in Pappalardo et al. (2004).

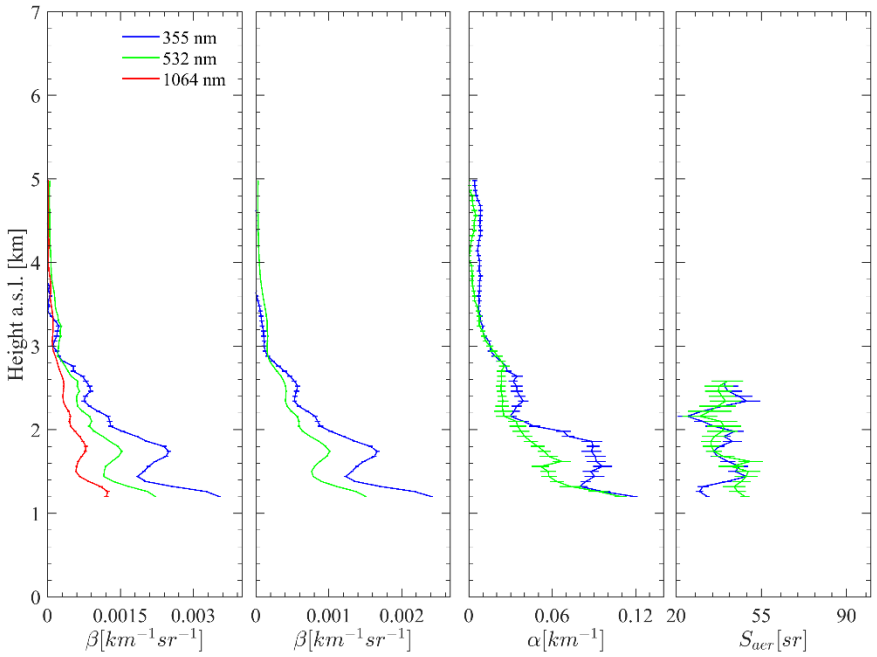

Figure F: *Optical profiles measured in Athens, on 22 May 2014, 20:28–21:28 UTC with a multiwavelength Raman lidar. From left to right, (a) the backscatter coefficient with the full resolution, (b) the smoothed backscatter coefficient, (c) the extinction coefficient, and (d) the lidar ratio. The error bars correspond to the standard deviation.*

References

Iarlori, M., Madonna, F., Rizi, V., Trickl, T., and Amodeo, A.: Effective resolution concepts for lidar observations, Atmos. Meas. Tech., 8, 5157-5176, https://doi.org/10.5194/amt-8-5157-2015, 2015.

Madonna, F., Amato, F., Vande Hey, J., and Pappalardo, G.: Ceilometer aerosol profiling versus Raman lidar in the frame of the INTERACT campaign of ACTRIS, Atmos. Meas. Tech., 8, 2207-2223, https://doi.org/10.5194/amt-8-2207-2015, 2015.

Mona, L., Papagiannopoulos, N., Basart, S., Baldasano, J., Binietoglou, I., Cornacchia, C., and Pappalardo, G.: EARLINET dust observations vs. BSC-DREAM8b modeled profiles: 12-year-long systematic comparison at Potenza, Italy, Atmospheric Chemistry and Physics, 14, 8781–8793, doi:10.5194/acp-14-8781-2014, 2014.

Ortiz-Amezcua, P., Guerrero-Rascado, J. L., Granados-Muñoz, M. J., Benavent-Oltra, J. A., Böckmann, C., Samaras, S., Stachlewska, I. S., Janicka, Ł., Baars, H., Bohlmann, S., and Alados-Arboledas, L.: Microphysical characterization of long-range transported biomass burning particles from North America at three EARLINET stations, Atmospheric Chemistry and Physics, 17, 5931–5946, doi:10.5194/acp-17-5931-2017, 2017.

Papagiannopoulos, N., Mona, L., Alados-Arboledas, L., Amiridis, V., Baars, H., Binietoglou, I., Bortoli, D., D'Amico, G., Giunta, A., Guerrero-Rascado, J. L., Schwarz, A., Perreira, S., Spinelli, N., Wandinger, U., Wang, X., and Pappalardo, G.: CALIPSO climatological products: evaluation and suggestions from EARLINET, Atmos. Chem. Phys., 16, 2341–2357, doi:10.5194/acp-16-2341-2016, 2016a.

Pappalardo, G., Amodeo, A., Pandolfi, M., Wandinger, U., Ansmann, A., Bösenberg, J., Matthias, V., Amiridis, V., De Tomasi, F., Frioud, M., Iarlori, M., Komguem, L., Papayannis, A., Rocadenbosch, F., and Wang, X.: Aerosol lidar intercomparison in the framework of the EARLINET project. 3. Raman lidar algorithm for aerosol extinction, backscatter, and lidar ratio, Appl. Opt., 43, 5370-5385. 2004.

Pappalardo, G., Mona, L., D'Amico, G., Wandinger, U., Adam, M., Amodeo, A., Ansmann, A., Apituley, A., Alados Arboledas, L., Balis, D., Boselli, A., Bravo-Aranda, J. A., Chaikovsky, A., Comeron, A., Cuesta, J., De Tomasi, F., Freudenthaler, V., Gausa, M., Giannakaki, E., Giehl, H., Giunta, A., Grigorov, I., Groß, S., Haeffelin, M., Hiebsch, A., Iarlori, M., Lange, D., Linné, H., Madonna, F., Mattis, I., Mamouri, R.-E., McAuliffe, M. A. P., Mitev, V., Molero, F., Navas-Guzman, F., Nicolae, D., Papayannis, A., Perrone, M. R., Pietras, C., Pietruczuk, A., Pisani, G., Preißler, J., Pujadas, M., Rizi, V., Ruth, A. A., Schmidt, J., Schnell, F., Seifert, P., Serikov, I., Sicard, M., Simeonov, V., Spinelli, N., Stebel, K., Tesche, M., Trickl, T., Wang, X., Wagner, F., Wiegner, M., and Wilson, K. M.: Four-dimensional distribution of the 2010 Eyjafjallajökull volcanic cloud over Europe observed by EARLINET, Atmos. Chem. Phys., 13, 4429-4450, https://doi.org/10.5194/acp-13-4429-2013, 2013.

Schwarz, A.: Aerosol typing over Europe and its benefits for the CALIPSO and EarthCARE missions - statistical analysis based on multiwavelength aerosol lidar measurements from ground-based EARLINET stations and comparison to spaceborne CALIPSO data, Ph.D. thesis, University of Leipzig, 2016.

Stein, A.F., Draxler, R.R, Rolph, G.D., Stunder, B.J.B., Cohen, M.D., and Ngan, F.: NOAA's HYSPLIT atmospheric transport and dispersion modeling system, Bull. Amer. Meteor. Soc., 96, 2059-2077, doi:10.1175/BAMS-D-14-00110.1, 2015.